

## Particle-driven gravity currents: asymptotic and box model solutions

Andrew J. Hogg<sup>1</sup>, Marius Ungarish<sup>2</sup>, Herbert E. Huppert<sup>3</sup>

*Institute of Theoretical Geophysics, Department of Applied Mathematics and Theoretical Physics, University of Cambridge,  
Silver Street, Cambridge CB3 9EW, UK*

(Received 28 April 1998; revised 3 March 1999; accepted 30 April 1999)

**Abstract** – We employ shallow water analysis to model the flow of particle-driven gravity currents above a horizontal boundary. While there exist similarity solutions for the propagation of a homogeneous gravity current, in which the density difference between the current and ambient is constant, there are no such similarity solutions for particle-driven currents. However, because the settling velocity of the particles is often much less than the initial velocity of propagation of these currents, we can develop an asymptotic series to obtain the deviations from the similarity solutions for homogeneous currents which describe particle-driven currents. The asymptotic results render significant insight into the dynamics of these flows and their domain of validity is determined by comparison with numerical integration of the governing equations and also with experimental measurements. An often used simplification of the governing equations leads to ‘box’ models wherein horizontal variations within the flow are neglected. We show how to derive these models rigorously by taking horizontal averages of the governing equations. The asymptotic series are then used to explain the origin of the scaling of these ‘box’ models and to assess their accuracy. © 2000 Éditions scientifiques et médicales Elsevier SAS

### 1. Introduction

Particle-driven gravity currents arise whenever suspensions of heavy particles are released into an ambient fluid. Because of the presence of the particles, the density of the suspension differs from that of the ambient and a buoyancy force is induced which drives the flow. However, during the evolution of the current, the particles continually sediment and are deposited from the flow, thus reducing the excess density of the suspension and the driving buoyancy force. There is hence significant coupling between the dynamics of the current and the transport of the particles. Particle-driven gravity currents occur naturally in the atmosphere, as a result of volcanic eruptions, for example; in the oceans, as a result of sediment-laden river outflows, for example; and in industrial settings, such as in the dumping of particle-rich pollutants.

There have been a number of previous studies of particle-driven gravity currents propagating above a horizontal surface which have provided experimental and theoretical understanding of the flows (Bonnecaze et al. [1,2]). These papers developed a model of the flow in which the buoyancy forces arising from the suspension of the relatively heavy particles are balanced by the inertial forces associated with the moving fluid (and viscous effects in the interior of the flow are neglected). The model utilizes the ‘shallow-water’ equations, which assume that the flow is predominantly horizontal and vertically uniform and that the pressure is hydrostatic. The current is assumed to intrude into the ambient with only negligible mixing across the interface between the two fluids. Particles are advected by the flow and settle out of the current through a basal viscous boundary

---

<sup>1</sup> Current address: Centre for Environmental and Geophysical Flows, School of Mathematics, University of Bristol, University Walk, Bristol BS8 1TW; email: a.j.hogg@bris.ac.uk

<sup>2</sup> Current address: Department of Computer Science, Technion, Haifa 32000, Israel; email: unga@csa.cs.technion.ac.il

<sup>3</sup> Correspondence and reprints; email: heh1@esc.cam.ac.uk

layer. At the front of the current, a Froude number condition is applied (Von Kármán [3], Benjamin [4], Huppert and Simpson [5]). This condition links the frontal velocity with the height and particle concentration. Bonnecaze et al. [1] formulated a theoretical description of the flow for two-dimensional currents flowing over smooth, horizontal surfaces and numerically integrated the resulting equations of motion. They found good agreement between their experimental observations and theoretical predictions. They were able not only to predict the frontal velocity for a given particle size and initial concentration, but also to compute accurately the deposit formed by the sedimentation from the flowing current. It should be emphasized that this model has no free parameters, other than those set externally by specifying the particular experiment. Bonnecaze et al. [2] performed a similar study of axisymmetric particle gravity currents and likewise found good agreement between experiments and theory.

A simplification of the shallow water equations describing the evolution of particle-driven gravity currents was proposed by Dade and Huppert [6] for an axisymmetric geometry and by Huppert and Dade [7] for two-dimensional situations. They formulated a ‘box model’ description of the flow, in which the properties of the current are assumed to be horizontally uniform. This class of models provide considerable insight into the dependency of the frontal velocity and deposit upon the size of the particles and their initial concentration. They also have the great, additional advantage of yielding analytical solutions. The scalings developed by Dade and Huppert [6] and Huppert and Dade [7] exhibit good agreement with the experimental data and are also borne out by the more rigorous numerical results of Bonnecaze et al. [1,2].

In the case of a vanishing settling velocity, the gravity current behaves like a constant density, compositional current, which has been widely studied (Huppert and Simpson [5]; Rottman and Simpson [8]). It has been shown in this case that release of a dense fluid within a less dense ambient attains a self-similar state independent of the details of the initial conditions (Chen [9], Grundy and Rottman [10]). The fundamentals of this similarity solution were first formulated by Hoult [11].

Analytical similarity solutions are advantageous tools for scientists and engineers. They provide both significant insight into the dynamical balances that govern the flow and exact results against which numerical codes may be tested. They also yield easily-calculated analytic expressions for the evolution of the dependent variables of any experimentally realisable situation. However, for a genuine particle-driven current, for which the settling velocity is non-zero, there is no self-similar evolution. Our purpose is to extend the benefits of the similarity solution to the particle-driven situation. We derive a perturbation correction to the similarity solution for constant density currents, reliant upon the small settling velocity of the particles. We find the leading order correction provides considerable insight into the evolution of the particle-driven gravity currents and brings out some of the noteworthy features of the numerical solutions of Bonnecaze et al. [1,2]. In addition, we are able to derive an expression for the position of the front of the current as a function of time which is in good agreement with experimental observations. We also include an appendix in which we utilise this asymptotic expansion to interpret more clearly the use of the analytically simplified box models.

We formulate the problem in Section 2 and introduce there the physical effects that govern the evolution of the current. In Section 3 we present the asymptotic analysis for a two-dimensional current based on an expansion which exploits the assumption that the settling velocity of the particles is much less than the initial speed of propagation of the current. We then compare the results with a numerical integration of the full system of equations. We draw some conclusions from this study in Section 4 and compare our analysis with the experimental observations of Bonnecaze et al. [1]. The paper also includes three appendices. In the first the results for the axisymmetric case are summarised. In the second we demonstrate how the same analytical framework may be used to study the two-layer model of Bonnecaze et al. [1]. This model accounts for the motion of the fluid overlying the gravity current and, in particular, we show how to justify the seemingly

counter-intuitive prediction that the overlying return flow leads to an increased frontal velocity of the current. In the third we examine the box model description of the flow in the light of this asymptotic analysis.

## 2. Formulation

Consider the intrusion of a suspension of particles over a horizontal boundary into a deep and quiescent ambient (*figure 1*). The ambient fluid is assumed to be of constant density,  $\rho_a$ , while the fluid making up the current is considered to be a suspension of monodispersed particles of density  $\rho_p$  and volume fraction  $\phi$ , with initial value  $\phi_0$ . We assume that the interstitial fluid of the suspension is the same as the ambient. (The industrially and naturally-occurring important case of relatively heavy particles suspended in light interstitial fluid was studied by Sparks et al. [12]. Application of the ideas expounded in this paper to that situation is straightforward.) We define the density parameter

$$\alpha = \frac{\rho_p - \rho_a}{\rho_a}. \quad (1)$$

The density of the suspension making up the current,  $\rho_c$ , is then given by

$$\rho_c = \rho_a(1 + \alpha\phi), \quad (2)$$

and the initial reduced gravity of the current is given by

$$g'_0 = \alpha\phi_0g, \quad (3)$$

where  $g$  is the gravitational acceleration. If the current is homogeneous and non-entraining, then the effective reduced gravity remains at its initial value  $g'_0$ . We note that in the analysis which follows, the normalised density difference between the fluid and particulate phases,  $\alpha$ , occurs only when multiplied by the gravitational acceleration and therefore the reduced gravity is the important parameter.

We employ a co-ordinate system (*figure 1*), with horizontal and vertical axes denoted by  $x$  and  $z$ , respectively. The current is of local height  $h$  and we formulate expressions for the conservation of mass, momentum and particles for the current, while the relatively deep ambient fluid is assumed to be quiescent. We assume that the dynamics of the current are governed by a balance of inertial and buoyancy forces and hence viscous effects may be neglected. (Bonnecaze et al. [1] found that in their experiments the dynamics of the particle-driven

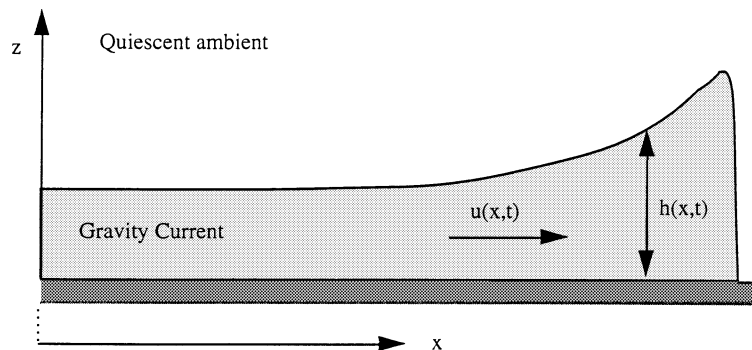


**Figure 1.** Schematic picture of a particle-laden gravity current flowing along a horizontal boundary, under a deep and otherwise quiescent ambient fluid.

gravity currents were indeed dominated by a balance of inertial and buoyancy forces. Ultimately viscous forces do play a role, but at this stage the current was almost arrested.) Additional physical effects which may occur with suspensions, as described, for example, by Ungarish [13], are negligible here because in the situations under consideration in this study both the relative velocity between the particulate and fluid phases and the initial volume fraction of particles are small. We employ the ‘shallow-water’ approximation for which the current itself is assumed to be in hydrostatic equilibrium in the vertical and the remaining governing equations are vertically averaged and reduced to expressions for the averaged horizontal velocity and volume fraction of particles, which are denoted by  $u$  and  $\phi$ , respectively. The shallow-water approach is based upon the current being of low aspect ratio and its velocity being predominantly horizontal. The variables which describes its evolution,  $u$ ,  $h$  and  $\phi$ , are considered as functions of the horizontal distance  $x$  and of time  $t$  only.

Following Einstein [14], Martin and Nokes [15] and Bonnecaze et al. [1], we assume that the dispersed particles sediment from the current only through a basal boundary layer with constant dimensionless settling velocity  $-\beta\hat{z}$ , where  $\hat{z}$  is a unit vector directed vertically upwards. The value of  $\beta$  may be calculated from the Stokes formula with the possible incorporation of hindrance (see Ungarish [13], for example). The turbulent intensity of the current is assumed to be sufficiently large to maintain the concentration profile vertically uniform, but insufficient to entrain deposited particles.<sup>1</sup>

In order to non-dimensionalise the equations, we first choose a suitable reference length,  $L_r$ . For the similarity solutions there is actually no ‘natural’ lengthscale; only the initial volume per unit width can be prescribed. We hence suggest defining a length scale for the two-dimensional case by

$$L_r = V_d^{1/2}, \quad (4)$$

where  $V_d$  is the initial volume of the current per unit perpendicular width. Reference velocity and time scales are then defined by

$$U_r = (L_r g'_0)^{1/2} \quad \text{and} \quad T_r = (L_r / g'_0)^{1/2}. \quad (5)$$

The particle volume fraction is scaled with  $\phi_0$ . The settling velocity of the particles is non-dimensionalised with respect to  $U_r$  (and is denoted by  $\beta$  as introduced above). This is taken to be a small parameter in the subsequent analysis. (Bonnecaze et al. [1] suggest a typical value of  $\beta$  as  $5 \times 10^{-3}$ . Note, however, that the velocity of propagation decays with time while the settling velocity of the particles is practically constant, hence even for small values of  $\beta$  the settling becomes important and even dominant. This is indeed pointed out by the following asymptotic expansion whose ‘small’ parameter is not  $\beta$ , but rather  $\beta$  multiplied by an increasing function of time.) The only additional parameter that explicitly enters the solution is the Froude number,  $Fr$ , at the front of the current which expresses the ratio of the velocity of propagation of the nose to the pressure head  $(g'h_N)^{1/2}$  (in dimensional form, where  $h_N$  is the height of the nose). The results obtained here are calculated for a current with  $Fr = 1.19$ , as semi-empirically determined by Huppert and Simpson [5], but may be straightforwardly extended to a current with a different value.

We note that a different choice of  $L_r$  does not affect the results derived below, even though its definition seemingly determines the magnitude of the dimensionless settling velocity  $\beta$ . We demonstrate that the perturbation to the similarity solution is not dependent upon any artificially defined lengthscale. We also discuss

---

<sup>1</sup> An alternative model of sedimentation has been formulated (Ungarish and Huppert [16]) in which it is assumed that there is laminar settling of the particles. The velocity of the particles relative to the suspending fluid is  $-\beta\hat{z}$  everywhere. The interface between the current and the ambient is defined by the kinematic shock which follows the boundary between the particles and the ‘pure fluid’ domain. By this process some of the interstitial fluid of the current is left behind the interface and becomes part of the embedding ambient fluid. The employment of such a model leads to results not very different from those derived here from the model for sedimentation from a turbulently moving fluid.

in Section 4 the simple connection between the present scaling and results and a prototype current released from a ‘lock’ with a reference length chosen as the initial height of the dense fluid.

### 3. Analysis

In this section we consider a two-dimensional, particle-laden gravity current and adopt a model of turbulent sedimentation from the flow. Following Bonnetcaze et al. [1], we write the dimensionless governing equations as

$$\frac{\partial h}{\partial t} + \frac{\partial}{\partial x}(uh) = 0, \quad (6)$$

$$\frac{\partial u}{\partial t} + u \frac{\partial u}{\partial x} + \phi \frac{\partial h}{\partial x} + \frac{h}{2} \frac{\partial \phi}{\partial x} = 0, \quad (7)$$

$$\frac{\partial \phi}{\partial t} + u \frac{\partial \phi}{\partial x} = -\frac{\beta \phi}{h}. \quad (8)$$

These are the expressions for the conservation of mass, momentum and particulate matter, respectively, for the gravity current. We note that for a vanishing settling velocity ( $\beta = 0$ ) and  $\phi = 1$ , the equations describing a compositional current are recovered (Huppert and Simpson [5]).

The equations are valid in the domain  $0 \leq x \leq x_N(t)$ , where  $x_N(t)$  is the dimensionless position of the front and are subject to the following boundary conditions, which are applied at all orders of the expansion described below. First, the volume of fluid which comprises the current is constant and is equal to the initial dimensionless volume  $\mathcal{V}_d$ , per unit width. This indicates that

$$\int_0^{x_N} h(x, t) dx = \mathcal{V}_d. \quad (9)$$

As discussed in the previous section, we introduce a dimensionless lengthscale which renders  $\mathcal{V}_d = 1$  for two-dimensional currents. A condition of no-flow at the rear wall yields

$$u(0, t) = 0. \quad (10)$$

A dynamic nose (or front) condition is required because the fluid motions there are three-dimensional and unsteady and hence can not be accurately reproduced by shallow water models. A number of studies have suggested that the velocity at the nose be related to the local wave velocity of the shallow water equations (Von Kàrmàn [3], Benjamin [4]) by

$$u(x_N, t) = Fr [h(x_N, t)\phi(x_N, t)]^{1/2}, \quad (11)$$

where  $Fr$  is the Froude number at the nose. Using inviscid fluid theory for a current of a constant excess density, moving within a deep ambient fluid, Benjamin [4] showed that  $Fr = \sqrt{2}$ . Huppert and Simpson [5] studied this condition experimentally for compositional currents and found that  $Fr = 1.19$ . The difference in values is due to the fact that at the nose viscous forces are not entirely negligible as the complex three-dimensional motions are dissipated. The Froude number of 1.19 has been successfully used to model experiments (Bonnetcaze et al. [1,2]). Finally, at the nose a kinematic condition is required, which is given by

$$\frac{d}{dt}x_N(t) = u(x_N, t). \quad (12)$$

We reiterate that these boundary conditions are applied at all orders of the asymptotic expansion developed below.

In general, initial conditions are required for the length, height and particle volume fraction in the current. We prescribe the initial value of the particle volume fraction as  $\phi = 1$ . However, the initial magnitudes for  $x_N$  and  $h$  cannot be prescribed to determine the similarity solution considered here, because this would introduce an additional lengthscale. Hence, in line with the usual way of determining similarity solutions, we prescribe the initial volume of the current but accept the need for the singular behaviour  $x_N \rightarrow 0$ ,  $h \rightarrow \infty$  at  $t \rightarrow 0$ .

When  $\beta = 0$  the equations of motion (6)–(8) and the aforementioned boundary conditions are satisfied by the classic similarity solution (Hoult [11])

$$x_N = Kt^{2/3}, \quad u = \frac{2}{3}Kt^{-1/3}U_0(y), \quad h = \frac{4}{9}K^2t^{-2/3}H_0(y) \quad \text{and} \quad \phi = 1, \quad (13)$$

where

$$y = x/Kt^{2/3}, \quad (14)$$

provided that

$$U_0(y) = y, \quad H_0(y) = \frac{1}{Fr^2} - \frac{1}{4} + \frac{1}{4}y^2 \quad \text{and} \quad K = \left( \frac{27Fr^2\mathcal{V}_d}{12 - 2Fr^2} \right)^{1/3}. \quad (15)$$

Note that in this solution we have not yet substituted  $\mathcal{V}_d = 1$  in order to indicate how the solution is changed by a different choice of non-dimensionalization. The validity of this solution may be verified by direct substitution, and will also be shown as a by-product of the subsequent analysis. Note that this theoretical prediction of the velocity of the front of the current has been confirmed experimentally (Huppert and Simpson [5]).

### 3.1. Asymptotic analysis

We extend this similarity solution to particle-driven currents by developing an asymptotic expansion which is valid for times such that  $t \ll (K^2/\beta)^{3/5}$ . Since  $\beta \ll 1$  we note that this corresponds to a considerable time span and hence the asymptotic series is a useful addition to the similarity solutions for the homogeneous currents. It is convenient to adopt the coordinate transformation (14) and consider  $h$ ,  $u$  and  $\phi$  as functions of  $y$  and  $t$ . The equations of motion in the new coordinates become

$$\frac{\partial h}{\partial t} + \left( K^{-1}t^{-2/3}u - \frac{2}{3}t^{-1}y \right) \frac{\partial h}{\partial y} + K^{-1}t^{-2/3}h \frac{\partial u}{\partial y} = 0, \quad (16)$$

$$\frac{\partial u}{\partial t} + \left( K^{-1}t^{-2/3}u - \frac{2}{3}t^{-1}y \right) \frac{\partial u}{\partial y} + K^{-1}t^{-2/3} \left( \phi \frac{\partial h}{\partial y} + \frac{1}{2}h \frac{\partial \phi}{\partial y} \right) = 0, \quad (17)$$

$$\frac{\partial \phi}{\partial t} + \left( K^{-1}t^{-2/3}u - \frac{2}{3}t^{-1}y \right) \frac{\partial \phi}{\partial y} = -\beta \frac{\phi}{h}. \quad (18)$$

The equations written in this form motivate the introduction of the variable

$$\tau = \beta K^{-2}t^{5/3}, \quad (19)$$

which will be used as the expansion parameter for the asymptotic series. The scaling of this parameter follows from a consideration of (18) in the regime  $\beta \ll 1$ . We substitute an expansion series in ascending powers of

$\beta$  for each of the dependent variables, using the similarity solution as the leading order terms. We find that  $\beta$  does not occur separately from  $K^{-2}t^{5/3}$  and so it is convenient to introduce the parameter  $\tau$  and propose the following expansions in the regime  $\tau \ll 1$ :

$$x_N = Kt^{2/3} [1 + \tau X_1 + \tau^2 X_2 + \dots], \quad (20)$$

$$u = \frac{2}{3} Kt^{-1/3} [U_0(y) + \tau U_1(y) + \tau^2 U_2(y) + \dots], \quad (21)$$

$$h = \frac{4}{9} K^2 t^{-2/3} [H_0(y) + \tau H_1(y) + \tau^2 H_2(y) + \dots], \quad (22)$$

$$\phi = 1 + \tau \varphi_1(y) + \tau^2 \varphi_2(y) + \dots, \quad (23)$$

where  $U_0(y)$  and  $H_0(y)$  are given by the similarity solution (15) and  $X_1, X_2$  are constants. Evidently, for  $\tau = 0$  ( $\beta = 0$ ) the similarity solution is recovered. We now demonstrate how to develop expansions which are consistent with both the equations of motion and the boundary conditions.

We substitute (21)–(23) into the equations of motion (16)–(18) and balance terms of equal powers of  $\tau$ . At  $O(1)$  the equations and boundary conditions are automatically satisfied, thus validating the similarity solution for  $\beta = 0$ . At  $O(\tau)$  the equations of continuity, momentum and particle transport yield, respectively,

$$5H_1 + 2(H_0U_1)' = 0, \quad (24)$$

$$3U_1 + H_1' + H_0'\varphi_1 + \frac{1}{2}H_0\varphi_1' = 0, \quad (25)$$

$$\varphi_1 = -\frac{27}{20} \frac{1}{H_0}, \quad (26)$$

where a prime denotes a derivative with respect to  $y$ . At  $O(\tau^2)$  the particle transport equation gives the relatively simple result

$$\varphi_2 = -\frac{27}{40} \frac{1}{H_0} \left( \varphi_1 - \frac{H_1}{H_0} \right) - \frac{1}{5} U_1 \varphi_1', \quad (27)$$

which is all we require from this order in this study.

We now consider the boundary conditions for these asymptotic series. First, we note that although the perturbation functions  $H_1(y), U_1(y)$ , etc. are defined in the domain  $0 \leq y \leq 1$ , the nose of the current is at

$$y_N = 1 + \tau X_1 + \tau^2 X_2 + O(\tau^3) \quad (28)$$

and  $y_N$  is expected to be smaller than unity. This follows because the current loses particles during its propagation and thus its effective buoyancy (and hence the driving force) decays with time. Hence its rate of propagation is also reduced.

The condition of no-flow at the origin (10) at  $y = 0$  is readily expressed as

$$U_1(0) = 0. \quad (29)$$

The dynamic condition at the nose (11), on account of the expansions (21)–(23) and (28), is rewritten as

$$U_0(1) + \tau X_1 U_0'(1) + \tau U_1(1) = Fr \{ [H_0(1) + \tau X_1 H_0'(1) + \tau H_1(1)] [1 + \tau \varphi_1(1)] \}^{1/2} [1 + O(\tau^2)]. \quad (30)$$

Expansion of both sides shows that the  $O(1)$  terms are balanced and the next order terms must satisfy

$$X_1 + U_1(1) = \frac{1}{2} [Fr^2 X_1 H_0'(1) + Fr^2 H_1(1) + \varphi_1(1)]. \quad (31)$$

The kinematic condition at the nose, (12), upon similar manipulation, reads

$$1 + \frac{7}{2} \tau X_1 + 6\tau^2 X_2 = U_0(1) + \tau X_1 U_0'(1) + \tau^2 X_2 U_0''(1) + \tau U_1(1) + \tau^2 X_1 U_1'(1) + \tau^2 U_2(1) + O(\tau^3) \quad (32)$$

resulting in at  $O(\tau)$

$$X_1 = \frac{2}{5} U_1(1), \quad (33)$$

and at  $O(\tau^2)$

$$X_2 = \frac{1}{6} [U_2(1) + U_1'(1) X_1]. \quad (34)$$

Finally, combining (31) and (33), we obtain

$$\frac{14 - Fr^2}{5} U_1(1) = Fr^2 H_1(1) + \varphi_1(1) \quad (35)$$

and after substitution of (25) and (26) this is reduced to a single, mixed boundary condition for the variable  $H_1$  only,

$$H_1(1) + \frac{14 - Fr^2}{15Fr^2} H_1'(1) = \frac{27}{20} \left[ 1 + \frac{14 - Fr^2}{60} \right]. \quad (36)$$

The solution of  $\varphi_1$ ,  $U_1$ ,  $H_1$ ,  $X_1$  and  $\varphi_2$  can now be obtained from (24)–(26) and (33) subject to the conditions (29) and (36). It follows immediately that  $\varphi_1$  is given explicitly by (26) and (15) as

$$\varphi_1(y) = -\frac{27}{20} / \left( \frac{1}{Fr^2} - \frac{1}{4} + \frac{1}{4}y^2 \right). \quad (37)$$

Substitution of this result into (25) and rearrangement give

$$U_1 = -\frac{1}{3} \left[ H_1' - \frac{27}{80}y / \left( \frac{1}{Fr^2} - \frac{1}{4} + \frac{1}{4}y^2 \right) \right], \quad (38)$$

and then subsequent substitution into (24) yields a second-order differential equation for  $H_1(y)$ , namely

$$\left( \frac{1}{Fr^2} - \frac{1}{4} + \frac{1}{4}y^2 \right) H_1'' + \frac{1}{2}y H_1' - \frac{15}{2} H_1 = \frac{27}{80}. \quad (39)$$

The boundary condition for  $H_1(y)$  at  $y = 1$  is provided by (36), while the other necessary constraint follows from (29) and (38) as

$$H_1'(0) = 0. \quad (40)$$

In essence these two boundary conditions are related to the dynamic condition at the nose and the condition of zero flow at the origin.

A numerical evaluation of  $H_1(y)$  and the subsequent calculation of  $U_1(y)$  and  $\varphi_1(y)$  is a straightforward task. However, we proceed here with an analytical solution. Upon the transformation of the independent variable,

$$\xi = iy \left( \frac{4}{Fr^2} - 1 \right)^{-1/2}, \tag{41}$$

where  $i = \sqrt{-1}$ , we find that (39) is reduced to

$$(1 - \xi^2) \frac{d^2}{d\xi^2} H_1 - 2\xi \frac{d}{d\xi} H_1 + 30H_1 = -\frac{27}{20}. \tag{42}$$

This is a standard Legendre equation (see, for example, Arfken and Weber [17]) and the solution can be expressed in terms of Legendre functions of order 5. On account of the condition (40) only the function of the second kind, denoted by  $Q_5$ , enters the result, which becomes

$$H_1(\xi) = C_T Q_5(\xi) - \frac{9}{200}. \tag{43}$$

The coefficient  $C_T$  is obtained from the boundary condition (36). It is real-valued but dependent on  $Fr$ . In particular,

$$C_T = -0.05623 \quad \text{for } Fr = 1.19. \tag{44}$$

Formally, this completes the solution for  $H_1(y)$ , from which  $U_1(y)$ ,  $X_1$  and  $\varphi_2(y)$  can be readily calculated. These functions are displayed in figures 2 and 3. In particular, we obtain

$$X_1 = -0.1809 \quad \text{for } Fr = 1.19. \tag{45}$$

Of major interest is the proportion of particles that have sedimented out of the current. This is defined by

$$S(t) = \frac{1}{\mathcal{V}_d} \int_0^{x_N} [1 - \phi(x, t)] h(x, t) dx, \tag{46}$$

where, again,  $\mathcal{V}_d$  is the initial dimensionless volume of the current. Using the asymptotic series developed above, we may evaluate  $S(t)$  with accuracy  $O(\tau^2)$  without calculating any further terms. In this way, we find that

$$\begin{aligned} S(\tau) &= -\frac{4 K^3}{9 \mathcal{V}_d} \int_0^{1+\tau X_1} (\tau \varphi_1 + \tau^2 \varphi_2)(H_0 + \tau H_1) dy + O(\tau^3) \\ &= -\frac{4 K^3}{9 \mathcal{V}_d} \left\{ \tau \int_0^1 H_0 \varphi_1 dy + \tau^2 \left[ \int_0^1 (H_1 \varphi_1 + H_0 \varphi_2) dy + H_0(1) \varphi_1(1) X_1 \right] \right\} + O(\tau^3) \\ &= \frac{3}{5} \frac{27 Fr^2}{12 - 2 Fr^2} (\tau - d_2 \tau^2) + O(\tau^3). \end{aligned} \tag{47}$$

Using the foregoing solution, we calculate that

$$d_2 = 1.183 \quad \text{for } Fr = 1.19. \tag{48}$$

Since  $S(\tau)$  must be an increasing function of  $\tau$ , (47) is valid at most up to  $\tau = 1/(2d_2)$ .

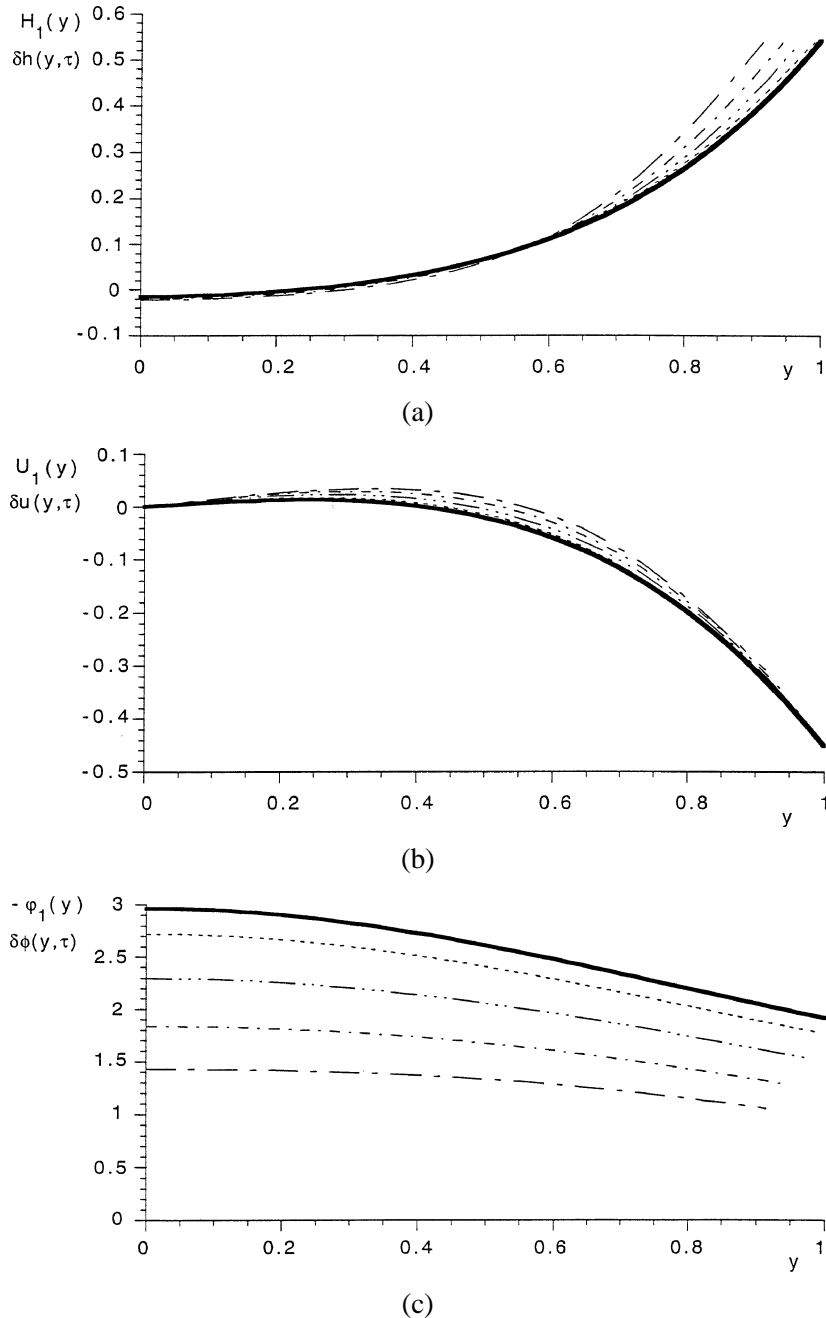


**Figure 2.** The first order asymptotic functions for (a) height  $H_1(y)$ ; (b) velocity  $U_1(y)$ ; and (c) (minus) volume fraction of particles  $-\varphi(y)$  of a two-dimensional current (—). Also plotted are the numerical evaluations of the normalised departure from the homogeneous similarity solution divided by  $\tau$ ,  $\delta h$ ,  $\delta u$  and  $\delta\phi$ , at  $\tau = 0.057$  (- - -),  $\tau = 0.18$  (- · · · -),  $\tau = 0.355$  (- · · · -) and  $\tau = 0.573$  (- - - - -).

Higher-order expansions may be derived in an analogous manner to the first-order expansions presented here. Using this technique, after lengthy algebraic manipulations, we computed the second-order terms in the power series expansions. In particular we find that  $X_2 = 0.06489$  for  $Fr = 1.19$ .

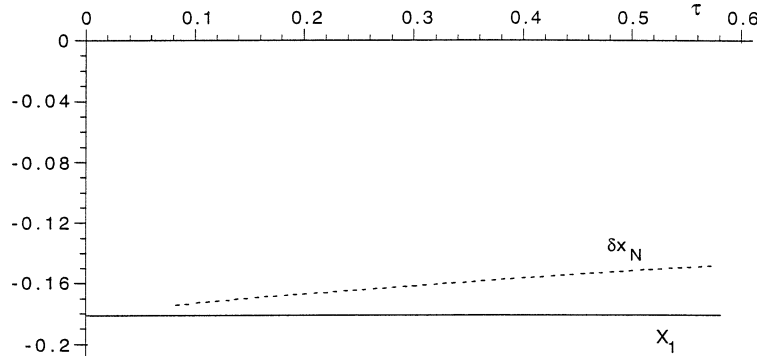


**Figure 3.** The first term in the asymptotic formulation of the normalised departure of the length of a two-dimensional, particle-driven current from the homogeneous similarity solution,  $X_1$ , (—). Also plotted is the numerical evaluation of this departure  $\delta x_N$  (- - - -).

### 3.2. Numerical solutions

These asymptotic series are compared with results arising from the numerical integration of the governing equations in order to assess further the validity of the analysis and the range of  $\tau$  for which the asymptotic expansion accurately reproduces the numerical results. For this purpose the governing equations, in terms of independent variables  $y$  and  $t$ , were recast into conservation form and discretised by a two-step Lax–Wendroff method, after the addition of an artificial viscosity to the momentum equation, which is necessary to damp spurious oscillations. (Similar methods have been described more fully by Bonnetcaze et al. [1,2], Ungarish and Huppert [16].) The initial conditions, however, were different from the usual ones employed to model lock-release gravity currents. To avoid a period of adjustment from the ‘lock-like’ initial conditions to the similarity solution which obscured the comparison with the asymptotic analysis, the dependent variables here were set equal to the form of the homogeneous similarity solution at the start of the numerical integration. However, this similarity solution is singular at  $t = 0$  ( $h \rightarrow \infty$ ). This difficulty was overcome by starting the integration at some small time  $t_0$ ; at this time, the initial conditions of  $h$ ,  $u$  and  $\phi$  were prescribed as the corresponding values in the similarity solution. We estimate that this produced a small deviation from the exact solution of  $O(\beta t_0^{5/3})$  and  $O(\beta t_0^2)$  for the two-dimensional and axisymmetric cases, respectively. This numerical scheme was employed for the analysis of both two-dimensional and axisymmetric currents with models of turbulent and laminar sedimentation. In a typical numerical integration, we used 200 grid points, a time step of  $5 \times 10^{-4}$  and an initial time of  $t_0 = 0.5$ . The dimensionless coefficient of artificial viscosity was 0.03.

We compare the asymptotic solutions with the numerical integration of the governing equations in the following stringent manner. We numerically evaluate the following expressions as functions of  $y$  and  $\tau$ :

$$\delta h(y, \tau) \equiv \frac{1}{\tau} \left[ \frac{h(y, t)}{(4/9)K^2 t^{-2/3}} - H_0(y) \right], \tag{49}$$

$$\delta u(y, \tau) \equiv \frac{1}{\tau} \left[ \frac{u(y, t)}{(2/3)K t^{-1/3}} - U_0(y) \right], \tag{50}$$

$$\delta \phi(y, \tau) \equiv \frac{1}{\tau} [1 - \phi(y, t)], \tag{51}$$

$$\delta x_N(\tau) \equiv \frac{1}{\tau} \left[ \frac{x_N(t)}{K t^{2/3}} - 1 \right]. \tag{52}$$

These expressions define functions which evaluate  $1/\tau$  times the departure of the normalised, numerically integrated solutions from the similarity solution for homogeneous gravity currents. As shown in figures 2

and 3, in the regime  $\tau \ll 1$  they are accurately represented by the leading-order asymptotics functions  $H_1(y)$ ,  $U_1(y)$ ,  $-\varphi_1(y)$  and  $X_1$ . However, as  $\tau$  increases, the functions  $\delta h$ ,  $\delta u$ ,  $\delta\phi$  and  $\delta x_N$  systematically depart from the first-order asymptotic solutions, suggesting the need to include higher-order terms in the asymptotic series.

The divergence between the numerical integration and the first-order asymptotic functions occurs most rapidly with the evaluation for the volume fraction of particles. We note that the use of only the first-order asymptotics becomes a poor approximation to the numerics at a relatively small value of  $\tau$  (figure 2(c)). For this dependent variable, however, we have also evaluated the second-order asymptotic function  $\varphi_2(y)$ . We compare the numerically evaluated function  $\delta\phi(y, \tau)$  with the leading two functions of the asymptotic series,  $-\varphi_1(y) - \tau\varphi_2(y)$ , in figure 4. This extended asymptotic series now accurately reproduces the numerics up to a much larger value of  $\tau$ . We also note that because we have calculated three terms in the asymptotic series of the volume fraction,  $\phi(y, \tau) = 1 + \tau\varphi_1(y) + \tau^2\varphi_2(y) + \dots$ , we may take a Shanks transform (Hinch [18]) to improve the convergence of the series. This further improves the agreement between the numerics and the asymptotics. Finally, we compare in figure 5 the numerical evaluation of the proportion of particles which have settled out of the current with the first two terms of the series expansion (47). We note that there is good

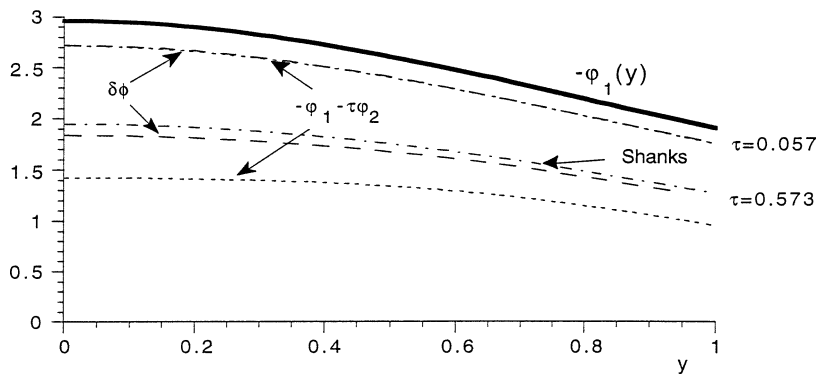


**Figure 4.** The sum of the leading two asymptotic functions for the volume fraction of a two-dimensional current,  $-\varphi_1(y) - \tau\varphi_2(y)$ , and the numerical evaluation of  $\delta\phi(y, \tau)$  as a function of  $y$  at various values of  $\tau$ . The graph shows the first-order asymptotic function  $-\varphi_1(y)$  (—); the numerical evaluation of the departure from the similarity solution,  $\delta\phi(y, \tau)$ , at  $\tau = 0.057$  and  $\tau = 0.573$  (---); the sum of the leading two asymptotic functions,  $-\varphi_1(y) - \tau\varphi_2(y)$ , at  $\tau = 0.057$  and  $\tau = 0.573$  (- - - -); and the Shanks transformation of the series for the volume fraction at  $\tau = 0.573$  (- · - · -).

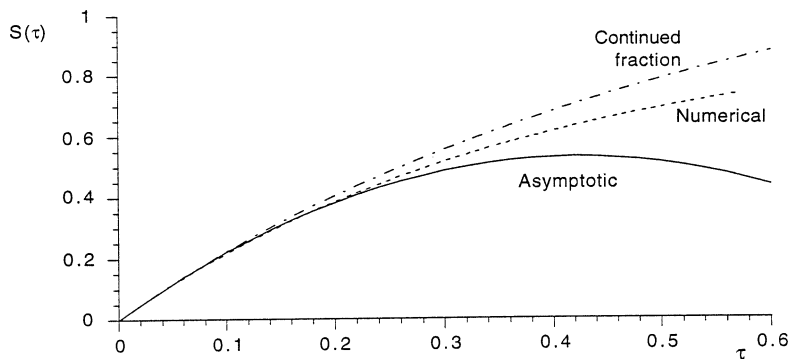


**Figure 5.** Comparison between the two-term asymptotic expression for the proportion of particles which have settled out of the current for a two-dimensional current,  $S(\tau)$ , and the numerical evaluation of this quantity as a function of  $\tau$ . The graph shows the asymptotic function (—), the numerical calculation (---) and the continued fraction approximant of the asymptotic series (- · - · -).

agreement between the two until approximately  $\tau = 0.3$ , after which the numerical and asymptotic functions diverge. We define this value of  $\tau$  as the limit of validity for our first-order asymptotic expansion. We also note that the use of a continued fraction approximant for the expansion of the proportion of particles within the current which have settled out of it, given by

$$S_{cf}(\tau) = \frac{3}{5} \frac{27Fr^2}{12 - 2Fr^2} \frac{\tau}{1 + d_2\tau}, \quad (53)$$

yields an improved estimate of the numerical calculation up to at least  $\tau = 0.6$ .

The extension of the above concepts to cover axisymmetric situations is presented in Appendix A.

#### 4. Discussion

We summarise in *table I* the asymptotic results derived in the preceding sections for two-dimensional and axisymmetric particle-driven gravity currents with laminar and turbulent models of sedimentation. The table presents the appropriate expansion parameter and the first-order asymptotic functions for the rate of propagation of the front of the current and the proportion of particles which have settled out of the current. It also provides a comparison with the ‘box’ model solutions and indicates a maximum value of the expansion parameter for which these asymptotic expressions adequately reproduce the numerically integrated solutions of the governing equations.

The form of the first-order asymptotic functions provide considerable insight into the dynamical balances within the flow and the way in which the evolution of particle-driven currents differ from homogeneous currents of the same initial excess density. The fundamental difference between the two is, of course, that the particles settle out of the flow to the underlying boundary. Hence the buoyancy of the current in the ambient is decreasing and thus the rate of propagation is also decreasing.

First, we consider the analysis of currents which are described using our model of turbulent sedimentation. (We observe by comparing *figures 2* and *7* that the qualitative forms of the first-order asymptotics for both the two-dimensional and axisymmetric currents are similar.) The first-order asymptotic function for the volume fraction of particles,  $\phi_1(y)$ , is always less than zero, indicating particle sedimentation along the entire length

**Table I.** The leading-order expressions for the position of the front and the proportion of settled particles for ‘box’ model and asymptotic series for two-dimensional particle-driven currents with models of both turbulent and laminar sedimentation and for axisymmetric particle-driven currents with a model of turbulent sedimentation. The series are calculated with  $Fr = 1.19$ .

		Two-dimensional		Axisymmetric
Sedimentation	Turbulent		Laminar	Turbulent
Expansion parameter		$\tau = \beta K^{-2} t^{5/3}$		$\sigma = \beta \kappa^{-2} t^2$
		$K = \left( \frac{27Fr^2 \gamma_d}{12 - 2Fr^2} \right)^{1/3}$		$\kappa = \left( \frac{32Fr^2 \gamma_a}{4 - Fr^2} \right)^{1/4}$
Asymptotic series				
Limit of validity	$\tau = 0.3$		$\tau = 0.4$	$\sigma = 0.15$
Position of front	$x_N = 1.61 K t^{2/3} (1 - 0.18\tau)$		$x_N = 1.61 K t^{2/3} (1 - 0.20\tau)$	$r_N = 1.54 \kappa t^{1/2} (1 - 0.18\sigma)$
Settled particles		$S(\tau) = 2.50\tau$		$S(\sigma) = 4.38\sigma$
Box models				
Position of front		$x_N = 1.47 K t^{2/3} (1 - 0.29\tau)$		$r_N = 1.72 \kappa t^{1/2} (1 - 0.29\sigma)$
Settled particles		$S(\tau) = 2.29$		$S(\sigma) = 3.52\sigma$

of the current. The reduction in the concentration of particles by sedimentation is greatest, though, at the tail of the current and least at the front. This distribution arises because the height of the tail is less than the height of the front. While the settling velocity of the individual particles is constant, the proportion of suspended particles which settle to the boundary is larger in the shallower regions of the current than in the deeper regions. The sedimentation of particles and the resultant reduction of the density difference between the current and ambient indicates that the velocity of propagation at the front is reduced relative to a current of constant excess density. Therefore we find that  $U_1 < 0$  near to  $y = 1$ . Within the current itself there exists an adverse pressure gradient which acts to slow down the fluid following the front of the current. Particle sedimentation affects this distribution of pressure in a complex way and leads to different effects in separate regions of the flow. Near to the origin, the pressure gradient resisting motion is reduced, the fluid accelerated and the height of the current reduced relative to that found within the similarity solution for homogeneous currents. Consequently, there is a region of fast moving, relatively particle-free fluid. Near to the front, however, the current is slowed relative to the homogeneous similarity solution and the height of the current is increased as fast-moving fluid from the tail piles up near to the nose.

These perturbation solutions have reflected a number of features of the structure of the flow noted by Bonnezaze et al. [1] from their numerical solutions. They observed a region near to the origin in which the volume fraction of particles is strongly depleted, the height of the current is significantly reduced and the flow is opposed by a relatively reduced pressure gradient. After a sufficient length of time, this developed into an internal bore which separated a particle-free, jet-like flow at the rear from a dense gravity-current-like flow at the front. We observe that the basis for the generation of this internal bore is to be found within the functional form of the first-order asymptotics, as described above.

In Section 2 we defined a lengthscale  $L_r$  which was used to non-dimensionalise the governing equations. We now demonstrate that the seemingly arbitrary choice of  $L_r$  does not affect the results derived here. This is most simply shown by verifying that the expansion parameter is independent of the choice of this lengthscale. Denoting the dimensional time by  $t'$ , we find that

$$\tau = \left( \frac{12 - 2Fr^2}{27Fr^2} \right)^{2/3} \frac{t'^{5/3} V_s g_0'^{1/3}}{V_d^{2/3}}, \quad (54)$$

where, again,  $V_s$ ,  $V_d$  and  $g_0'$  are the dimensional particle settling velocity, the initial volume of the current (per unit width) and the initial reduced density of the current fluid, respectively. Thus the choice of lengthscale used to render the problem dimensionless does not play a role in the asymptotic expansions developed in this study. The influence of the particles on the behaviour of the current, according to the asymptotic expansions developed in this study, depends on the volume of the current (per unit width),  $V_d$ , but not on the particular initial geometry. This, however, is subject to the following restriction.

In practice a typical constant volume current is produced by a lock release. Hence, in the two-dimensional analysis, the initial conditions for shallow water equations are not those employed in Section 3, but rather

$$u = 0, \quad \phi = 1 \quad \text{and} \quad h = h_0 \quad \text{for} \quad 0 \leq x \leq \mathcal{V}_d/h_0, \quad (55)$$

where  $h_0$  is the initial dimensionless height of the lock. There is both computational and experimental evidence that although these conditions are different from the similarity shape, the current is well approximated by the similarity solution after an initial slumping period ( $t_{sl} \approx 3x_0/h_0^{1/2}$ ). Substituting  $t_{sl}$  in (19) yields  $\tau_{sl}$  which is expected to be the lower bound of the interval  $\tau$  for which the present approximation is valid. Thus, the initial aspect ratio of the lock-released current determines the range of validity of the expansion, but not the results. Evidently, our results are of practical value only when  $\tau_{sl} \ll 1$  which is equivalent to the statement that during

the slumping phase only a small fraction of the dispersed particles sediment to the underlying boundary. This condition, though, is not restrictive as we illustrate by use of the experimental data of Bonnecaze et al. [1].

Bonnecaze et al. [1] experimentally studied the gravity currents which arose when suspensions of silicon carbide particles were released into pure water. The density of these particles,  $\rho_p$  is  $3.22 \text{ g cm}^{-3}$ , and the experiments employed particles with mean diameters, 9, 23, 37 and  $53 \mu\text{m}$ , while the initial volume fraction of particulate was in the range of 1–4%. We estimate the timescale of slumping for flows with an initial reduced gravity,  $g'_0$ , of  $22.9 \text{ cm s}^{-2}$ , released from a lock of length 15 cm and height 30 cm. Thus the slumping time,  $t_{sl}$ , is 1.7 s. On the other hand, we have demonstrated that the expansions of Section 3 are valid up to an approximate minimum value of  $\tau = 0.5$ . This corresponds to dimensional times of 116, 38, 21 and 14 s, for particles of the particles of diameter 9, 23, 37 and  $53 \mu\text{m}$ , respectively. There are thus significant times during which the behaviour of the current is accurately modelled by the theoretical model presented here.

Bonnecaze et al. [1] developed a shallow-water description of the current which, when integrated numerically, was able to accurately model the evolution of the flow. Their model is identical to that employed here with the additional feature that the return flow within the ambient fluid overlying the current was accounted for. We demonstrate in Appendix B that the influence of the return flow is  $O(t^{-2/3})$  and hence it has progressively less effect on the propagation of the current. Therefore our analysis, which neglects the influence of the ambient fluid, will become increasingly accurate as time progresses. We compare the experimental data of Bonnecaze et al. [1] with our analytical expression for the propagation of the front of the current (20). It is convenient to re-scale the experimentally measured position of the front and time with respect to a lengthscale,  $L_p$ , and a timescale,  $T_p$ , given by

$$L_p = \left[ \frac{V_d(g'_0 V_d)^{1/2}}{V_s} \right]^{2/5} \quad \text{and} \quad T_p = \frac{V_d}{V_s L_p}. \quad (56)$$

Denoting the dimensionless position of the front by  $\mathcal{L}$  and dimensionless time by  $\mathcal{T}$ , we re-plot the experimental data of Bonnecaze et al. [1] in *figure 6*. (Note that these new dimensionless variables are related to those of Section 3 by  $\mathcal{L} = x_N \beta^{2/5}$  and  $\mathcal{T} = (\tau K^2)^{3/5}$ .) We observe that in terms of these new dimensionless variables the experimental data for four particle sizes, three initial volume fractions and three volumes of the current per unit width are collapsed onto each other. The eight data series displayed in *figure 6* span the range of experimental conditions investigated by Bonnecaze et al. [1]. In terms of the asymptotic theory developed here, we note that

$$\mathcal{L}(\mathcal{T}) = K \mathcal{T}^{2/3} \left( 1 + \frac{X_1}{K^2} \mathcal{T}^{5/3} + \frac{X_2}{K^4} \mathcal{T}^{10/3} + \dots \right), \quad (57)$$

where  $K \equiv [27Fr^2/(12 - 2Fr^2)]^{1/3} = 1.6$  for  $Fr = 1.19$ . In *figure 6* we plot the first-order approximation and note that it accurately reproduces the experimental data up to  $\mathcal{T} \approx 2$ . Thereafter the first-order approximation rapidly diverges from the theoretical prediction. We also show the continued fraction representation of the first order expansion and note that this slightly extends the domain in which it accurately models the experimental data. The final curve plotted in *figure 6* is the [1, 1] Padé approximant of the second-order expansion. We observe that this accurately reproduces the experimental observations over the entire range of measurements. We have thus avoided the need for the numerical integration of a system of partial differential equations and instead have derived an analytical expression for the rate of propagation of the front of the current, which is in excellent agreement with the experimental data.

We conclude that the asymptotic analysis developed here has permitted a number of the valuable characteristics of the similarity solutions for homogeneous gravity currents to be carried over to particle-driven currents. We have developed analytical expressions for the first-order asymptotic functions in both

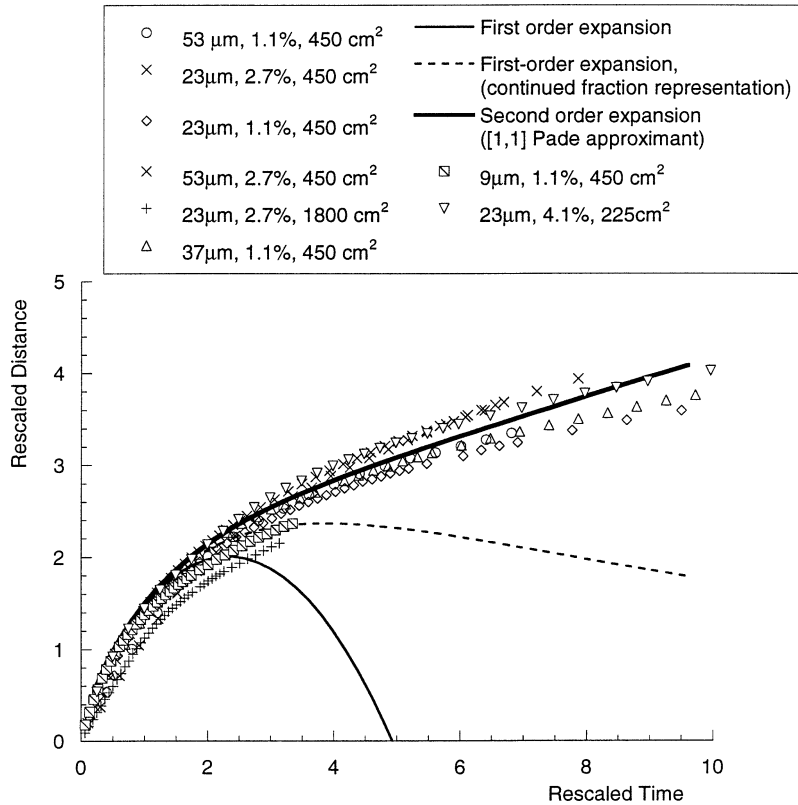


**Figure 6.** Comparison between the asymptotic theory and the experimental results of Bonnecaze et al. [1] for the position of the front of the current as a function of time. The particle size, initial volume fraction and volume of fluid per unit width for each of the data series are listed in the legend.

two-dimensional and axisymmetric geometries (the latter in Appendix A). These functions yield significant insight into the structure of the solutions to the governing equations and the various dynamical effects. By comparison with numerical solutions of the governing equations and with experiments, we identify the regime for which these first-order expansions are valid.

Finally in Appendix C, we have demonstrated how to derive rigorously from the full shallow-water equations box model solutions which neglect horizontal variations. We have been able to suggest why such solutions provide a possibly more reasonable than expected model of the dynamics.

### Appendix A. Axisymmetric currents

We analyse the evolution of particle-driven axisymmetric currents and derive a correction to the similarity solution for homogeneous currents. The analysis closely follows the approach of the preceding sections for two-dimensional currents, although the details of the calculation are somewhat different. We employ a cylindrical coordinate system  $r$ ,  $\theta$ ,  $z$ , and  $u$  now represents the vertically averaged velocity component in the radial direction. The azimuthal velocity component is identically zero and we consider a flow which exhibits only temporal and radial dependence. The analysis also applies to a flow in a sector of constant angle. The dimensionless equations describing the evolution of the current were derived by Bonnecaze et al. [2] and are given by

$$\frac{\partial h}{\partial t} + \frac{1}{r} \frac{\partial}{\partial r}(ruh) = 0, \quad (\text{A1})$$

$$\frac{\partial u}{\partial t} + u \frac{\partial u}{\partial r} + \phi \frac{\partial h}{\partial r} + \frac{1}{2} h \frac{\partial \phi}{\partial r} = 0, \quad (\text{A2})$$

$$\frac{\partial \phi}{\partial t} + u \frac{\partial \phi}{\partial r} = -\beta \frac{\phi}{h}. \quad (\text{A3})$$

The equations are valid in the domain  $0 \leq r \leq r_N(t)$ , where  $r_N$  is the dimensionless position of the front of the current. The boundary conditions are analogous to those for a two-dimensional current and are given by

$$\int_0^{r_N} h(r, t) r dr = \mathcal{V}_a, \quad (\text{A4})$$

$$u(0, t) = 0, \quad (\text{A5})$$

$$u(r_N, t) = Fr [\phi(r_N, t) u(r_N, t)]^{1/2}, \quad (\text{A6})$$

$$\frac{d}{dt} r_N = u(r_N, t), \quad (\text{A7})$$

where  $\mathcal{V}_a$  is the dimensionless initial volume of the current. These equations represent the integral expression for the global conservation of volume (A4); vanishing velocity at the origin (A5); the dynamic condition at the front of the current (A6); and the kinematic condition at the front (A7). This system of equations has been numerically integrated by Bonnecaze et al. [2] and has been shown to exhibit excellent agreement with experimental observations.

As for two-dimensional currents, there exists a similarity solution for non-entraining, axisymmetric gravity currents of constant excess density ( $\beta = 0$ ) and we derive the asymptotic correction to this expression in the regime of small settling velocity ( $\beta \ll 1$ ). The similarity solution was first calculated by Hoult [11] and takes the form

$$r_N = \kappa t^{1/2}, \quad u = \frac{1}{2} \kappa t^{-1/2} \mathcal{U}_0(\eta), \quad h = \frac{1}{4} \kappa^2 t^{-1} \mathcal{H}_0(\eta) \quad \text{and} \quad \phi = 1, \quad (\text{A8})$$

where

$$\eta = r / \kappa t^{1/2}, \quad \kappa = \left( \frac{32 Fr^2 \mathcal{V}_a}{4 - Fr^2} \right)^{1/4}, \quad (\text{A9})$$

and

$$\mathcal{U}_0(\eta) = \eta, \quad \mathcal{H}_0(\eta) = \frac{1}{Fr^2} - \frac{1}{2} + \frac{1}{2} \eta^2. \quad (\text{A10})$$

It has been shown that compositional currents are well modelled by this similarity form of solution after a sufficient lapse of time from their initiation (Bonnecaze et al. [2]).

As before, it is convenient to adopt the coordinate transformation (A9) and consider  $h$ ,  $u$  and  $\phi$  functions of  $\eta$  and  $t$ . The equations of motion become

$$\frac{\partial h}{\partial t} + \left( \kappa^{-1} t^{-1/2} u - \frac{1}{2} t^{-1} \eta \right) \frac{\partial h}{\partial \eta} + \kappa^{-1} t^{-1/2} \left( h \frac{\partial u}{\partial \eta} + \frac{uh}{\eta} \right) = 0, \quad (\text{A11})$$

$$\frac{\partial u}{\partial t} + \left( \kappa^{-1} t^{-1/2} u - \frac{1}{2} t^{-1} \eta \right) \frac{\partial u}{\partial \eta} + \kappa^{-1} t^{-1/2} \left( \phi \frac{\partial h}{\partial \eta} + \frac{1}{2} h \frac{\partial \phi}{\partial \eta} \right) = 0, \quad (\text{A12})$$

$$\frac{\partial \phi}{\partial t} + \left( \kappa^{-1} t^{-1/2} u - \frac{1}{2} t^{-1} \eta \right) \frac{\partial \phi}{\partial \eta} = -\beta \frac{\phi}{h}. \quad (\text{A13})$$

We define the variable

$$\sigma = \beta \kappa^{-2} t^2, \quad (\text{A14})$$

which will be utilised as a small parameter in the analysis which follows. We introduce the expansions

$$r_N = \kappa t^{1/2} [1 + \sigma R_1 + \sigma^2 R_2 + \dots], \quad (\text{A15})$$

$$u = \frac{1}{2} \kappa t^{-1/2} [\mathcal{U}_0(\eta) + \sigma \mathcal{U}_1(\eta) + \sigma^2 \mathcal{U}_2(\eta) + \dots], \quad (\text{A16})$$

$$h = \frac{1}{4} \kappa^2 t^{-1} [\mathcal{H}_0(\eta) + \sigma \mathcal{H}_1(\eta) + \sigma^2 \mathcal{H}_2(\eta) + \dots], \quad (\text{A17})$$

$$\phi = 1 + \sigma \psi_1(\eta) + \sigma^2 \psi_2(\eta) + \dots. \quad (\text{A18})$$

Again, we substitute these expansions into the governing equations (A11)–(A13) and balance terms of equal powers of  $\sigma$ . At  $O(1)$ , the terms are already in balance by virtue of the similarity solution. At  $O(\sigma)$ , we obtain the following expressions for the conservation of fluid volume, momentum and the transport of particles, respectively,

$$(\mathcal{H}_0 \mathcal{U}_1)' + 4\mathcal{H}_1 + \mathcal{H}_0 \mathcal{U}_1 / \eta = 0, \quad (\text{A19})$$

$$\mathcal{H}'_1 + 4\mathcal{U}_1 - \eta / \mathcal{H}_0 = 0, \quad (\text{A20})$$

$$\psi_1 = -2 / \mathcal{H}_0, \quad (\text{A21})$$

where a prime is used now to denote differentiation with respect to  $\eta$ . At  $O(\sigma^2)$  we consider only the result of the particle conservation equation, which is a function of variables at lower order and is given by

$$\psi_2 = -\frac{1}{\mathcal{H}_0} \left( \psi_1 - \frac{\mathcal{H}_1}{\mathcal{H}_0} \right) - \frac{1}{8} \mathcal{U}_1 \psi'_1. \quad (\text{A22})$$

The corresponding boundary conditions, in terms of these perturbation functions, are that at the origin there is no flow and so

$$\mathcal{U}_1(0) = 0, \quad (\text{A23})$$

which, on account of (A20), also imposes

$$\mathcal{H}'_1(0) = 0. \quad (\text{A24})$$

The dynamic nose condition (A6) renders at  $O(\sigma)$

$$\mathcal{U}_1(1) + R_1 \left[ 1 - \frac{1}{2} Fr^2 \mathcal{H}'_0(1) \right] = \frac{1}{2} Fr^2 \mathcal{H}_1(1) + \frac{1}{2} \psi_1(1). \quad (\text{A25})$$

The kinematic nose condition (A7) yields

$$R_1 = \frac{1}{4} \mathcal{U}_1(1) \quad \text{and} \quad R_2 = \frac{1}{8} [\mathcal{U}_2(1) + \mathcal{U}'_1(1) R_1]. \quad (\text{A26})$$

The combination of these results provides a single mixed boundary condition of  $\mathcal{H}_1$ :

$$\mathcal{H}_1(1) + \frac{10 - Fr^2}{16 Fr^2} \mathcal{H}'_1(1) = 2 + \frac{10 - Fr^2}{16}. \quad (\text{A27})$$

The solution  $\psi_1(y)$  emerges in a straightforward fashion from (A21) and (A10) and we then solve the remaining governing equations (A19) and (A20) subject to the boundary conditions (A24) and (A27). We eliminate  $\mathcal{U}_1$  from these equations to obtain

$$\eta \left( \frac{1}{Fr^2} - \frac{1}{2} + \frac{1}{2}\eta^2 \right) \mathcal{H}_1'' + \left( \frac{1}{Fr^2} - \frac{1}{2} + \frac{3}{2}\eta^2 \right) \mathcal{H}_1' - 16\eta \mathcal{H}_1 = 2\eta. \quad (\text{A28})$$

A change of variable, given by

$$\zeta = -\frac{Fr^2}{2 - Fr^2\eta^2}, \quad (\text{A29})$$

reduces (A28) to an inhomogeneous hypergeometric equation (see Arfken and Weber [17])

$$\zeta(1 - \zeta) \frac{d^2 \mathcal{H}_1}{d\zeta^2} + (1 - 2\zeta) \frac{d\mathcal{H}_1}{d\zeta} + 8\mathcal{H}_1 = -1. \quad (\text{A30})$$

The solution, which satisfies the boundary condition at  $\zeta = 0$  (A24), is

$$\mathcal{H}_1(\zeta) = C_A {}_2F_1(a, b, 1; \zeta) - \frac{1}{8}, \quad (\text{A31})$$

where  $a = (1 + \sqrt{33})/2$ ,  $b = (1 - \sqrt{33})/2$  and the coefficient  $C_A$  is determined by the boundary condition (A27). In particular,

$$C_A = 0.09044 \quad \text{for } Fr = 1.19. \quad (\text{A32})$$

The remaining unknowns  $\mathcal{U}_1(\eta)$ ,  $\psi_2(\eta)$  and  $R_1$  follow straightforwardly from  $\mathcal{H}_1(\eta)$  and  $\psi_1(\eta)$  by (A20), (A22) and (A26), respectively. Results are displayed in *figures 7* and *8*, and, in particular,

$$R_1 = -0.1754 \quad \text{for } Fr = 1.19. \quad (\text{A33})$$

The proportion of particles which have settled from the current may be calculated from

$$\mathcal{S}(\sigma) = \frac{1}{\mathcal{V}_a} \int_0^{r_N} (1 - \phi) h r dr. \quad (\text{A34})$$

Using our expansions for the leading terms, we obtain

$$\mathcal{S}(\sigma) = -\frac{8Fr^2}{4 - Fr^2} \left\{ \sigma \int_0^1 \psi_1 \mathcal{H}_0 \eta d\eta + \sigma^2 \left[ \int_0^1 (\psi_2 \mathcal{H}_0 + \psi_1 \mathcal{H}_1) \eta d\eta - 2R_1 \right] \right\} + \mathcal{O}(\sigma^3) \quad (\text{A35})$$

$$= \frac{8Fr^2}{4 - Fr^2} [\sigma - k_2 \sigma^2] + \mathcal{O}(\sigma^3), \quad (\text{A36})$$

where

$$k_2 = 2.638 \quad \text{for } Fr = 1.19. \quad (\text{A37})$$

We compare these asymptotic solutions with numerical integration of the governing equations in an analogous manner to Section 3. From the numerical solutions we evaluate the following functions to measure

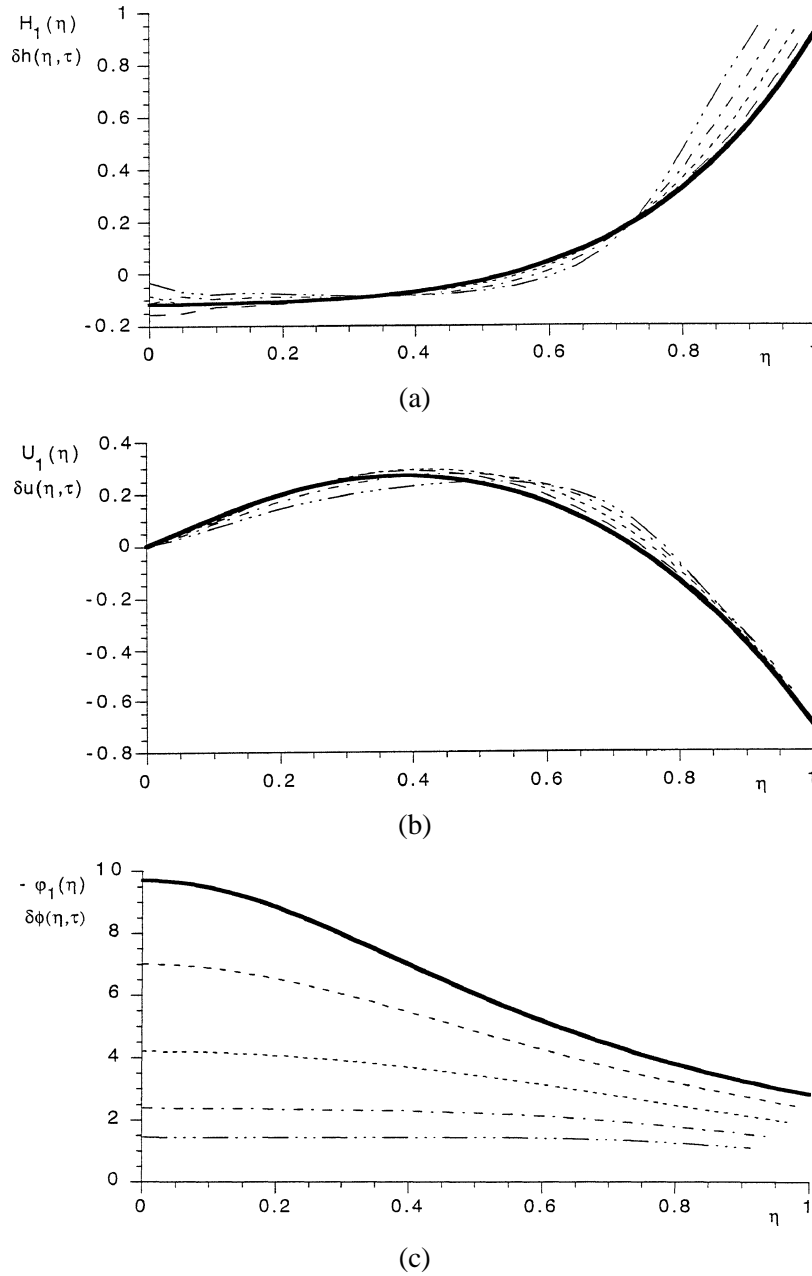


**Figure 7.** The first-order asymptotic functions for (a) height  $H_1(\eta)$ ; (b) velocity  $U_1(\eta)$ ; and (c) (minus) volume fraction of particles  $-\varphi(\eta)$  of an axisymmetric current (——). Also plotted are the numerical evaluation of the normalised departure from the homogeneous similarity solution divided by  $\sigma$ ,  $\delta h$ ,  $\delta u$  and  $\delta\phi$ , at  $\sigma = 0.076$  (-----),  $\sigma = 0.21$  (.....),  $\sigma = 0.41$  (-·-·-) and  $\sigma = 0.68$  (—·—·—·—·—).

the departure from the similarity solutions for a homogeneous current

$$\delta h(\eta, \sigma) = \frac{1}{\sigma} \left[ \frac{h(\eta, t)}{(1/4)\kappa^2 t^{-1}} - \mathcal{H}_0(\eta) \right], \tag{A38}$$

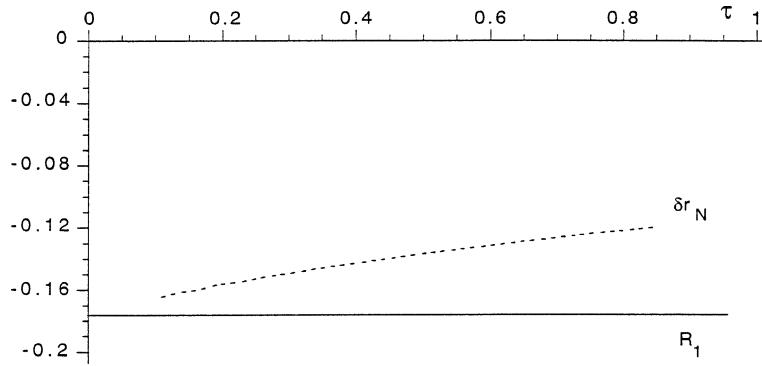


**Figure 8.** The first term in the asymptotic formulation of the normalised departure of the length of an axisymmetric, particle-driven current from the homogeneous similarity solution (—),  $R_1$ . Also plotted is the numerical evaluation (---) of this departure  $\delta r_N$ .

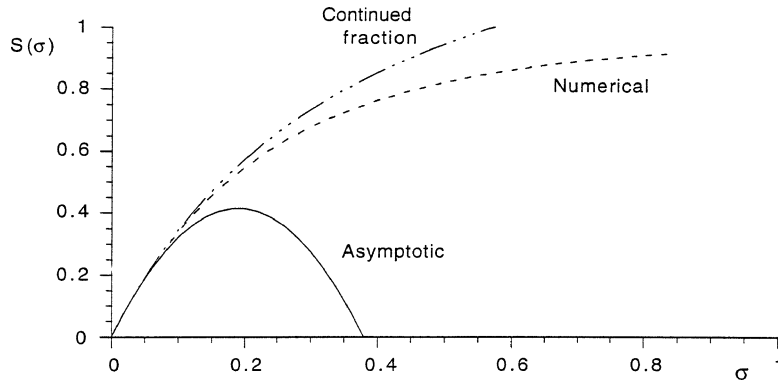


**Figure 9.** Comparison between the two-term asymptotic expression for the proportion of particles which have settled out of the current for an axisymmetric current,  $S(\sigma)$ , and the numerical evaluation of this quantity as a function of  $\sigma$ . The graph shows the asymptotic function (—), the numerical calculation (---) and the continued fraction approximation of the asymptotic series (— · — · — · —).

$$\delta u(\eta, \sigma) = \frac{1}{\sigma} \left[ \frac{u(\eta, t)}{(1/2)\kappa t^{-1/2}} - \mathcal{U}_0(\eta) \right], \tag{A39}$$

$$\delta \phi(\eta, \sigma) = \frac{1}{\sigma} [1 - \phi(\eta, t)], \tag{A40}$$

$$\delta r_N(\sigma) = \frac{1}{\sigma} \left[ \frac{r_N(t)}{\kappa t^{1/2}} - 1 \right]. \tag{A41}$$

These are plotted on the same graphs as the first-order asymptotic functions  $\mathcal{H}_1(\eta)$ ,  $\mathcal{U}_1(\eta)$ ,  $-\psi_1(\eta)$  and  $\sigma R_1$  at various values of  $\sigma$  in figures 7 and 8. Once again we observe good agreement between the asymptotics and the numerics, with the expected gradual divergence of the two as  $\sigma$  increases, which indicates the need to include higher-order corrections. Again the divergence of the numerical solutions from the first-order asymptotics is most pronounced for the volume fraction of particles (figure 7(c)), which is relatively poorly represented by its first-order asymptotic function. We compare the numerical and two-term asymptotic evaluation of the proportion of particles which have settled out of the current in figure 9. We note that there is good agreement until around  $\sigma = 0.15$ , at which point approximately 40% of the particles have settled out of the current. We take this value of  $\sigma$  as the definition of the limit of validity of our first-order expansion.

## Appendix B. Two-layer model

In this appendix we consider the flow of a non-entraining gravity current of constant density as it propagates over a horizontal boundary under an ambient fluid which is sufficiently shallow so that its motion cannot be neglected. As the current passes, a return flow is set up within the ambient as a consequence of mass continuity. It is assumed that there is no interfacial drag between the two layers and that the flows are vertically uniform. Such a model of two-layer flow has been successfully employed by a series of studies (Rottman and Simpson [8]; Bonnetcaze et al. [1]; Hallworth et al. [19]) and has been found to explain some features of the flow which are unresolved by single-layer models. We consider here a two-dimensional gravity current and employ the length and time scales  $L_r$  and  $T_r$ , given by (4) and (5), to render the variables dimensionless. We denote the height and velocity of the upper layer by  $h_u$  and  $u_u$ , respectively, while as in Section 3 the height and velocity of the current are denoted by  $h$  and  $u$ . We further simplify the problem by assuming that the combined height of the current and overlying ambient is constant and is denoted by  $H$ . The equations of mass continuity in each layer are given by

$$\frac{\partial h}{\partial t} + \frac{\partial}{\partial x}(uh) = 0, \quad (\text{B1})$$

$$\frac{\partial h_u}{\partial t} + \frac{\partial}{\partial x}(u_u h_u) = 0, \quad (\text{B2})$$

whilst the momentum equations in each layer are

$$\frac{\partial}{\partial t}(uh) + \frac{\partial}{\partial x}(u^2 h + h^2/2) + h \frac{\partial p_i}{\partial x} = 0, \quad (\text{B3})$$

$$\frac{\partial}{\partial t}(u_u h_u) + \frac{\partial}{\partial x}(u_u^2 h_u) + h_u \frac{\partial p_i}{\partial x} = 0, \quad (\text{B4})$$

where  $p_i$  is the pressure at the interface between the fluids. Since the combined depth of the current and ambient is constant ( $h + h_u = H$ ) and the volume fluxes of fluid in each layer balance ( $uh + u_u h_u = 0$ ), we may eliminate the interfacial pressure from (B3) to find (Hallworth et al. [19])

$$\frac{\partial}{\partial t}(uh) + (1 - h/H) \frac{\partial}{\partial x}(u^2 h + h^2/2) - \frac{h}{H^2} \frac{\partial}{\partial x} \left( \frac{u^2 h^2}{1 - h/H} \right) = 0. \quad (\text{B5})$$

We analyse this equation, together with (B1) in the regime  $\varepsilon \equiv 1/H \ll 1$ . These equations are applicable along the length of the current and we denote the position of the front by  $x_N(t)$ . The boundary conditions are given by

$$u(0, t) = 0, \quad (\text{B6})$$

$$\frac{dx_N}{dt} = u(x_N, t), \quad (\text{B7})$$

$$u(x_N, t) = Fr [h(x_N, t)]^{1/2}, \quad (\text{B8})$$

$$\int_0^{x_N} h dx = 1. \quad (\text{B9})$$

These equations represent the condition of no flow at the origin (B6); the kinematic condition at the front of the current (B7); the dynamic condition at the front (B8); and the global conservation of fluid volume (B9). We may not specify initial conditions in an analogous manner to Section 3 because this would imply that at  $t = 0$  the height of the current would exceed the total depth of fluid,  $H$ . Instead we require that our solution

for the two-layer flow recovers the similarity solution of the single-layer as  $t \rightarrow \infty$ . This similarity solution is given by (13). We recast the governing equations in terms of  $y$  and  $t$ , using the coordinate transformation given by (14). A convenient parameter for the asymptotic expansions of the height, velocity and position of the front is given by

$$\lambda = \varepsilon K^2 t^{-2/3}. \quad (\text{B10})$$

In the regime  $\lambda \ll 1$ , we propose the following series

$$x_N = K t^{2/3} [1 + \lambda X_1 + \dots], \quad (\text{B11})$$

$$u = \frac{2}{3} K t^{-1/3} [U_0(y) + \lambda U_1(y) + \dots], \quad (\text{B12})$$

$$h = \frac{4}{9} K^2 t^{-2/3} [H_0(y) + \lambda H_1(y) + \dots]. \quad (\text{B13})$$

The leading-order solutions are the similarity solutions for the single-layer model of a gravity current. At  $O(\lambda)$  we obtain

$$-H_1 + (H_0 U_1)' = 0, \quad (\text{B14})$$

$$-\frac{1}{3} U_1 + \frac{2}{3} H_1' = \frac{8}{27} (U_0^2 H_0 + H_0^2/2)', \quad (\text{B15})$$

where a prime denotes differentiation with respect to  $y$ . We now formulate the boundary conditions for these first-order asymptotic functions. This analysis proceeds in a manner analogous to Section 3. Hence we find that the condition of no-flow at the origin yields

$$U_1(0) = 0. \quad (\text{B16})$$

The kinematic condition at the nose leads to

$$U_1(1) + X_1 = 0 \quad (\text{B17})$$

and the dynamic condition at the nose gives

$$H_1(1) + X_1 H_0'(1) = 0. \quad (\text{B18})$$

We eliminate the velocity perturbation  $U_1$  from (B14) and (B15) to yield the following equation:

$$(H_0 H_1')' - H_1/2 = \frac{4}{9} [H_0 (U_0^2 H_0 + H_0^2/2)]'. \quad (\text{B19})$$

Upon the transformation of the independent variable to  $\zeta = iy(4/Fr^2 - 1)^{-1/2}$ , we find that this equation becomes a standard Legendre equation with homogeneous solutions of Legendre functions of order 1. On account of the boundary condition (B16), we find that only the Legendre function of the second kind, which we denote by  $Q_1(\zeta)$ , enters this solution. Hence we find that

$$H_1(\zeta) = A Q_1(\zeta) + \left( \frac{1}{Fr^2} - \frac{1}{4} \right)^2 \left( \frac{20}{9} \zeta^4 - \frac{8}{3} \zeta^2 + \frac{4}{9} \right). \quad (\text{B20})$$

The remaining constant,  $A$ , is determined from the boundary conditions. As in Section 3, it is real and dependent upon the magnitude of the Froude number at the front of the current. We find that

$$A = 0.5860 \quad \text{for } Fr = 1.19. \quad (\text{B21})$$

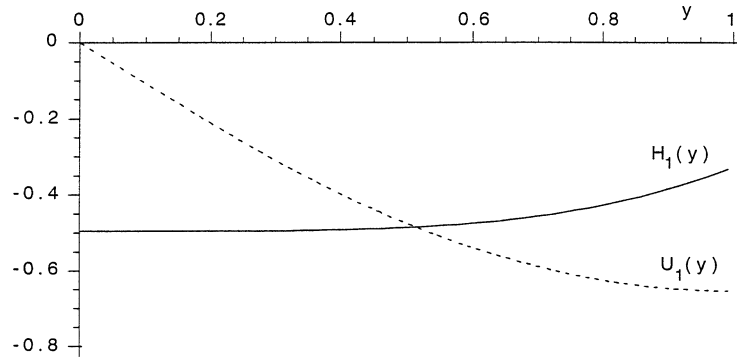


**Figure 10.** The first-order asymptotic functions for (a) height  $H_1(y)$  (—); and (b) velocity  $U_1(y)$  (- - -) in a two layer model of a homogeneous two-dimensional gravity current.

This implies that  $X_1 = 0.6540$ . We plot the functions  $H_1(y)$  and  $U_1(y)$  in *figure 10*. We note that the effect of including the motion of the upper layer is to accelerate the gravity current ( $X_1 > 0$ ). This is a somewhat counter-intuitive result because the ambient flow is in opposition to the flow of the gravity current. However interfacial drag, which would act to decelerate the gravity current, is not included in this simple model of the motion. Instead the distribution of the interfacial pressure is such that the flow accelerates. There is some evidence of this behaviour in the numerical results of Bonnecaze et al. [1]. They found that it was necessary to include the motion of the ambient fluid in order to model accurately their experimental results. We also note that the extra velocity of the current decays with increasing time as  $t^{-2/3}$ , because as the current spreads out and becomes thinner, the return flow within the ambient is reduced. Thus, the behaviour of the solution is represented by the single-layer similarity solution with increasing accuracy as time advances.

### Appendix C. Derivation of the box model

In this appendix we illuminate the conditions for the validity of the analytical ‘box’ models of gravity currents that have been proposed by Huppert and Simpson [5], Dade and Huppert [6] and Huppert and Dade [7] and also show how they can be determined from the full governing equations. For box models horizontal variations in the properties of the current are neglected. The resulting analysis, however, leads to accurate predictions of the scaling dependencies of the frontal velocity. Box models may be formulated for both axisymmetric and two-dimensional currents. In this appendix, however, we focus only on two-dimensional currents. (Axisymmetric currents can be similarly analysed.) Starting from the shallow-water equations (Eqs (6)–(8)), we consider the horizontally-integrated expressions for the conservation of mass, momentum and particles which are given by

$$\frac{d}{dt} \int_0^{x_N} h dx = 0, \quad (\text{C1})$$

$$\frac{d}{dt} \int_0^{x_N} hu dx = - \left[ \frac{1}{2} h^2 \phi \right]_0^{x_N}, \quad (\text{C2})$$

$$\frac{d}{dt} \int_0^{x_N} h\phi dx = -\beta \int_0^{x_N} \phi dx. \quad (\text{C3})$$

The boundary conditions for these equations are given by (9)–(12). For the ‘box’ models, we solve for the temporal variation of the frontal position and the height and volume fraction at the front; we do not explicitly solve for the height and velocity ‘within’ the current. This implies that the momentum condition (C2) is not

required since the velocity at the boundary is specified by the Froude number condition,

$$\frac{dx_N}{dt} = Fr[\phi(x_N, t)h(x_N, t)]^{1/2}. \quad (C4)$$

We now make the following substitutions which link the integrals of the properties of the current to the conditions at the front. We write

$$\int_0^{x_N} h dx = f_1(t)x_N h(x_N, t), \quad (C5)$$

$$\int_0^{x_N} h\phi dx = f_2(t)x_N h(x_N, t)\phi(x_N, t), \quad (C6)$$

$$\int_0^{x_N} \phi dx = f_3(t)x_N \phi(x_N, t), \quad (C7)$$

where each of  $f_1(t)$ ,  $f_2(t)$ ,  $f_3(t)$  are functions of time. If the current evolves in a self-similar manner then these functions are constants, because there are constant ratios of the average height and volume fraction of particles to their values at the nose of the current. The magnitude of these ratios indicate the skewness of the distribution within the current; if the currents were truly box-like then the value of these ratios would be unity. If, however, the current does not evolve in a self similar manner, then  $f_1(t)$ ,  $f_2(t)$ ,  $f_3(t)$  will not be constant.

In the limit  $\beta = 0$ , the current is a non-entraining, gravity current of constant density. There exists a similarity solution for such flows, which was given in Section 3. In this case we find that

$$f_1 = f_2 = 1 - \frac{1}{6}Fr^2, \quad f_3 = 1. \quad (C8)$$

We observe that  $f_1, f_2 < 1$  which is consistent with the height of a self-similar homogeneous gravity current being skewed towards the nose.

When  $\beta$  is non-zero, there is no similarity form of solution and the functions  $f_1(t)$ ,  $f_2(t)$ ,  $f_3(t)$  are not necessarily constant. We employ the perturbation analysis of Section 3 to evaluate series expansions for each of these functions. In the regime  $\tau \equiv \beta K^{-2}t^{5/3} \ll 1$  and with  $Fr = 1.19$ , we find that

$$f_1(\tau) = 0.76(1 - 0.47\tau + \dots), \quad (C9)$$

$$f_2(\tau) = 0.76(1 - 1.1\tau + \dots), \quad (C10)$$

$$f_3(\tau) = 1 - 0.63\tau + \dots. \quad (C11)$$

In the limit  $\tau = 0$  and with  $Fr = 1.19$ , these expressions are equivalent to (C8). We note that the form of each of the functions implies that the distribution of fluid and particulate mass becomes increasing skewed towards the nose, a conclusion which is borne out in the results of both the asymptotic and numerical analysis of the shallow-water equations. We recall from Section 3 that these first-order solutions are valid until approximately  $\tau = 0.5$ , within which range of values each of these exhibits a considerable variation in value. Box models which utilise the assumption that these distribution functions are constant, have been formulated by Dade and Huppert [6], Bonnetcaze et al. [2] and Hallworth et al. [19] to find the rate of propagation of the currents and the resulting deposit. These ‘box’ model solutions provide not only the dimensionless ratios of parameters on which the characteristics of the current depends, but also the relevant functional dependency upon the dimensionless time and downstream distance. All that is undetermined is a series of constants, which correspond to the values ascribed to the functions  $f_1(t)$ ,  $f_2(t)$  and  $f_3(t)$ . It is to be expected that the values of these should differ from unity since the distributions of height and volume fraction of particles throughout the current are non-uniform.

In the analysis which follows, we work through the ‘box’ model approach and attempt to justify its success in reproducing predictions from more complex numerical models.

The ‘box’ model approach yields

$$h_{NxN} f_1 = \mathcal{V}_d, \quad (\text{C12})$$

$$\frac{d}{dt}(f_2 h_{NxN} \phi_N) = -\beta f_3 \phi_N x_N, \quad (\text{C13})$$

together with the Froude number condition at the front (C4), where we have used a suffix of  $N$  to indicate the function evaluated at the nose of the current. Hence, substituting  $\Phi = f_2 \phi_N / f_1$  into (C12) and (C13), we find that

$$\frac{d\Phi}{dt} = -\frac{\beta f_3 f_1}{f_2 \mathcal{V}_d} \Phi x_N, \quad (\text{C14})$$

$$\frac{dx_N}{dt} = Fr \left( \frac{\mathcal{V}_d \Phi}{x_N f_2} \right)^{1/2}. \quad (\text{C15})$$

We note that all of the parameters within the box model may be removed from these two governing equations by the adoption of new non-dimensional variables. We introduce new dimensionless variables for the frontal position and time, denoted by  $L$  and  $T$ , respectively, which have been rendered dimensionless by  $L_\infty$  and  $T_\infty$ , which are given by

$$L_\infty = \left( \frac{5Fr(g'_p \phi_0)^{1/2} V_d^{3/2}}{V_s} \right)^{2/5} \quad \text{and} \quad T_\infty = \frac{5V_d}{V_s L_\infty}. \quad (\text{C16})$$

In these expressions,  $V_s$  denotes the dimensional settling velocity of the particles. The box model dimensionless time is related to the expansion parameter  $\tau$  by

$$\tau = 5K^{-2} Fr^{-2/3} T^{5/3}. \quad (\text{C17})$$

It turns out that just as the asymptotic expansions of Section 3 could be expressed in power series of  $\tau$ , so the box model variables can be expressed in power series of  $T^{5/3}$ . These two variables,  $L$  and  $\Phi$ , are simply related by a function of the Froude number at the front of the current. The adoption of this new non-dimensionalisation renders the ‘box’ model equations as

$$\frac{d\Phi}{dT} = -\frac{f_3 f_1}{f_2} \Phi L, \quad (\text{C18})$$

$$\frac{dL}{dT} = \left( \frac{\Phi}{L f_2} \right)^{1/2}. \quad (\text{C19})$$

Integration of the model is based upon the assumption that the ratios of the shape functions,  $f_3 f_1 / f_2$  and  $f_2^{-1/2}$ , are constant and equal to unity, for simplicity. While we noted above that individually these functions are not constant, we find that when they are combined in these ratios they exhibit a substantial weaker variation. The ratios of the functions may be expanded as the following series:

$$\frac{f_3 f_1}{f_2} = 1 - 0.045\tau + \dots, \quad (\text{C20})$$

$$f_2^{-1/2} = 1.14(1 + 0.53\tau + \dots). \quad (\text{C21})$$

Using the box model equations, it is also possible to derive simple relationships for the temporal evolution of length of the current and the proportion of particles which have settled out of the current (Hallworth et al. [19]).

By expanding such relationships in the regime  $T \ll 1$  and using (C17) to write these expansions in terms of  $\tau$ , we may compare the box model results with the asymptotic analysis of the shallow-water equations. In *table I*, we present a summary of these results, expanded up to  $O(\tau^2)$  with  $Fr = 1.19$ . We find that the agreement between the box model analysis and the asymptotic treatment of the full governing equations is reasonable and in some ways remarkable given the restrictive assumptions of the theory which underlies the box model approach. Box models, however, may be applied at large times which is a significant advantage over the first-order asymptotic analysis developed here.

## Acknowledgements

The financial support of the Ministry of Agriculture, Fisheries and Food (UK) and EPSRC is gratefully acknowledged. AJH acknowledges the financial support of a grant from the Nuffield Foundation. MU acknowledges the support of The Fund for Promotion of Research at the Technion.

## References

- [1] Bonnecaze R.T., Huppert H.E., Lister J.R., Particle-driven gravity currents, *J. Fluid Mech.* 250 (1993) 339–369.
- [2] Bonnecaze R.T., Hallworth M.A., Huppert H.E., Lister J.R., Axisymmetric particle-driven gravity currents, *J. Fluid Mech.* 294 (1995) 93–121.
- [3] Kármán, T. Von, The engineer grapples with nonlinear problems, *Bull. Am. Math. Soc.* 46 (1940) 615–683.
- [4] Benjamin T.B., Gravity currents and related phenomena, *J. Fluid Mech.* 88 (1968) 223–240.
- [5] Huppert H.E., Simpson J.E., The slumping of gravity currents, *J. Fluid Mech.* 99 (1980) 785–799.
- [6] Dade W.B., Huppert H.E., A box model for non-entraining suspension-driven gravity surges on horizontal surfaces, *Sedimentology* 42 (1995) 453–471.
- [7] Huppert H.E., Dade W.B., Natural disasters: explosive volcanic eruptions and gigantic landslides, *Theor. Comput. Fluid Dynam.* 10 (1998) 201–212.
- [8] Rottman J.W., Simpson J.E., Gravity currents produced by instantaneous releases of heavy fluid in a rectangular channel, *J. Fluid Mech.* 135 (1983) 95–100.
- [9] Chen J.C., Studies on gravitational spreading currents, PhD thesis, California Institute of Technology, 1980.
- [10] Grundy R.E., Rottman J.W., The approach to self-similarity of the solutions of the shallow-water equations representation gravity current releases, *J. Fluid Mech.* 156 (1985) 39–53.
- [11] Hoult D.P., Oil spreading on the sea, *Annu. Rev. Fluid Mech.* 2 (1972), 341–368.
- [12] Sparks R.S.J., Bonnecaze R.T., Huppert H.E., Lister J.R., Hallworth M.A., Mader H., Phillips J.C., Sediment-laden gravity currents with reversing buoyancy, *Earth Planet. Sc. Lett.* 114 (1993) 243–257.
- [13] Ungarish M., *Hydrodynamics of Suspensions*, Springer-Verlag, 1993, p. 317.
- [14] Einstein H., Deposit of suspended particles in a gravel bed, *J. Hydraul. Div.-ASCE* 94 (1968) 1197–1205.
- [15] Martin D., Nokes R., Crystal settling in a vigorously convecting magma chamber, *Nature* 332 (1988) 543–536.
- [16] Ungarish M., Huppert H.E., The effects of rotation on axisymmetric particle-driven gravity currents, *J. Fluid Mech.* 362 (1998) 17–51.
- [17] Arfken G.B., Weber H.J., *Mathematical Methods for Physicists*. Edition IV, Academic Press, 1995, p. 1029.
- [18] Hinch E.J., *Perturbation Methods*, Cambridge University Press, 1992, p. 160.
- [19] Hallworth M.A., Hogg A.J., Huppert H.E., Effects of uniform flow on compositional and particle gravity currents, *J. Fluid Mech.* 359 (1998) 109–142.